AAS 23-129

ARTEMIS I OFF-NOMINAL-TRAJECTORY DESIGN AND OPTIMIZATION

Robert E. Harpold,* Colin Brown,† Brian J. Killeen,‡ Randy A. Eckman,§ Timothy F. Dawn,¶ Badejo Adebonojo,‖ Jacob Williams**

In order to achieve the Artemis I mission objectives to human-rate the Orion spacecraft even under off-nominal conditions, trajectories were developed to handle contingency scenarios: alternate missions for contingencies before or during the Trans-Lunar Injection burn, recoveries to return Orion to the nominal trajectory after a delayed or partial burn, and abort trajectories to return the spacecraft to Earth after a critical failure. In addition, disposal trajectories were generated for situations where recovery was not an option. Details are given on the trajectory characteristics, solution families, the generation of the trajectories, and operations considerations.

INTRODUCTION

The Artemis program has a goal of returning people to the Moon, which will involve, at a minimum, the Space Launch System (SLS) rocket, the Orion spacecraft, and the Human Landing System (HLS). Artemis I tested the SLS and Orion systems to ensure they were sufficient for human use. The Artemis I mission objectives[1] were, from highest priority to lowest:

- Demonstrate Orion heat shield performance at lunar-return velocities.
- Operate vehicle systems in flight environment.
- Retrieve Orion Crew Module.
- Complete remaining objectives.

A flight plan was developed in order to achieve these objectives. Trajectory-related contingency scenarios were defined for the flight in order to achieve as many high-priority objectives as possible in off-nominal situations. In some cases, these contingencies would have returned Orion to the nominal trajectory. In other cases, they would have been alternate missions, would have returned Orion early without achieving all the desired objectives, or would have disposed of Orion to prevent it from becoming a hazard. This paper will introduce the types of trajectory-related contingency scenarios for Artemis I, discuss how the corresponding trajectories were generated, and discuss the results.

*ERC Inc., Houston, TX 77058
†Barrios, Houston, TX 77058
‡EG/Aeroscience and Flight Mechanics, NASA Johnson Space Center, Houston, TX 77058
§EG/Aeroscience and Flight Mechanics, NASA Johnson Space Center, Houston, TX 77058
¶EG/Aeroscience and Flight Mechanics, NASA Johnson Space Center, Houston, TX 77058
‖Jacobs Technology, Houston, TX 77058
**EG/Aeroscience and Flight Mechanics, NASA Johnson Space Center, Houston, TX 77058

TOOLS AND MODELS

A software tool called Copernicus was used in conjunction with a tool called Damocles to run Copernicus in parallel to generate thousands of trajectories. These tools, as well as the models used for the trajectories, are described in the following sub-sections.

Copernicus

The primary tool for mission analysis and design for Artemis I was the Copernicus generalized trajectory-design and optimization system,[2,3] created by Cesar Ocampo and now developed at NASA's Johnson Space Center (JSC), which allows the user to optimize arbitrary trajectories in a flexible multiple-shooting-type framework. Copernicus includes a Graphical User Interface (GUI) and integrated 3D trajectory visualization, as well as Python scripting components. The user constructs a trajectory as a collection of segments, each of which include user-defined properties (such as time, mass, state, engine parameters, and maneuver controls) that can be specified, inherited from another segment, or optimized and constrained. The user can choose from several optimizers and propagators, the latter of which can be specified for each segment. For Artemis I planning, the Sparse Nonlinear Optimizer (SNOPT)[4] was chosen as the optimizer, and the DDEABM Adams-Bashforth-Moulton variable step-size, variable-order method[5] was used as the propagator.

Damocles

A wrapper program called Damocles[6] was written to run many Copernicus scans in parallel. A nominal-trajectory scan consisted of trajectories being generated for launch periods throughout a year, all days within those launch periods, and integer-minute intervals throughout those launch windows, which resulted in trajectories for thousands of epochs. If a given trajectory failed a mission constraint, such as an eclipse violation, Damocles attempted to mitigate the violation and achieve a usable trajectory.

For each successfully solved nominal mission, corresponding to a single launch epoch, separate scans generated off-nominal trajectories as an N-dimensional matrix of trajectory-parameter combinations, where N is the number of trajectory parameters for a particular off-nominal scenario. For example, to define a post-TLI abort trajectory, the following parameters are needed: the number of abort burns, the time of ignition of the first abort burn, the abort-burn engines, the entry-interface day, etc. This approach of a parametric sweep of trajectories resulted in a broad and complete dataset, as opposed to targeted analysis to determine bounding scenarios that might not be flown operationally.

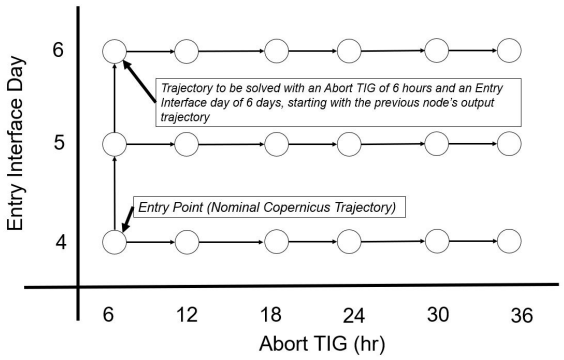

Figure 1: Example Damocles Rooted Polytree

The combinations of scan parameters were treated as the nodes of a Directed Acyclic Graph (DAG) (Figure 1). The graph nodes were connected with directed edges by parsing the user-provided dependencies. For example, if the user provides a scan parameter called `ABORT TIG` and also defines a dependency on the same parameter (i.e., `ABORT TIG dependent on previous`

`ABORT TIG`), Damocles would sequentially solve aborts, increasing the Time of Ignition (TIG) by a provided time delta. Each sequential solution would start from the previous solution. Any number of dependencies can be provided, as long as a priority is provided as well for each dependency. The priority determines which nodes are connected, which in practice determines the path of sequential solution (i.e,. along scan parameter A or scan parameter B). If the user does not provide any dependencies, the problem is massively parallelizable. For a set of off-nominal cases, the initial case would be solved and then used as a seed for other nodes in the DAG.

Due to the massive scale of trajectories being produced, analysts used NASA JSC's Flight Sciences Laboratory high-performance-computer cluster and the Amazon Web Services GovCloud clusters to run Damocles with the SLURM job-scheduling system. For each off-nominal trajectory case, Damocles would:

1. Extract the relevant nominal Artemis I trajectories from a previous Damocles scan.
2. Parse a user's inputs, such as off-nominal-trajectory type, scan parameters, dependency parameters, and a Python script to edit, solve, and post-process the off-nominal trajectory.
3. Compute a series of the rooted polytrees for the off-nominal-trajectory scenario (one polytree per nominal trajectory).
4. Submit a SLURM job to execute the rooted polytrees.
5. Solve each node per the rooted polytree and the user-provided Python script.
6. The results were compressed and returned to a shared network where analysts used the results to determine the off-nominal capability of the vehicle for those particular launch epochs.

When allocating workers on a computing cluster, Damocles used exclusive nodes so the SLURM job would use all the available CPUs on that node, which allowed many cases to run in parallel on a single machine. This approach meant all trajectories for a particular launch epoch would be solved on that node, which meant there would be no dependency between launch epochs for the off-nominal scans.

Trajectory Models

Earth, Moon, and Sun state vectors were extracted from the JPL DE421 ephemeris.[7] Spherical-harmonic gravity modeling was used for the dominant central body for each segment, with the remaining two celestial bodies modeled as point masses. For mission phases near Earth, the Gravity Recovery And Climate Experiment (GRACE) GGM02C Earth gravity model[8] was used, truncated to degree and order 8×8. The Earth-fixed frame was resolved using the classical equinox-based FK5 reductions defined by the IAU 1976/1980/1982/1994 models implemented in the Standards of Fundamental Astronomy (SOFA).[9] In the mission-design phase, all Earth Orientation Parameters were assumed to be zero except for $\Delta\mathrm{UT1} = 0.1\ \mathrm{sec}$. During the mission, the values were set using real-time International Earth Rotation Service (IERS) Standard Rapid EOP Data `finals.all`. For lunar gravity, the Gravity Recovery and Interior Laboratory (GRAIL) GRGM660PRIM model[10] was used, truncated to degree and order 50×50 in lunar-flyby segments, 4×4 for segments in the Distant Retrograde Orbit (DRO), and 8×8 elsewhere. The lunar Principal Axis frame was used as the body-fixed frame for gravity models, while the Mean Earth/Polar Axis was assumed for geodetic parameters.[11]

NOMINAL TRAJECTORY

The nominal trajectory[6] (Figure 2) can be broken into several phases:

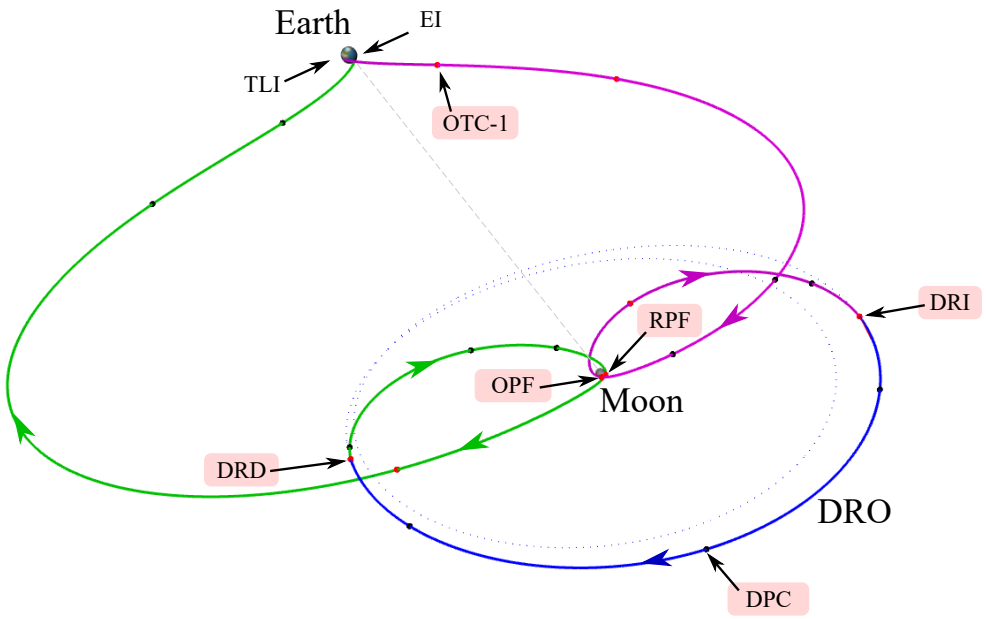

Figure 2: Artemis I reference trajectory for the 2022-11-16 0634 UTC launch, with the major burns labeled (Earth-Moon Two-Body Rotating Pulsating Frame).

1. Ascent to Trans-Lunar Injection (TLI): The spacecraft launches, enters Earth orbit, and uses the Interim Cryogenic Propulsion Stage (ICPS) to perform TLI to coast to the Moon.
2. TLI to Outbound Powered Flyby (OPF): The spacecraft coasts to the Moon and performs the OPF burn.
3. OPF to DRO Insertion (DRI): The spacecraft coasts to the insertion point of the DRO and performs the DRI burn.
4. DRI to DRO Plane Change (DPC): The spacecraft is in a DRO $\sim$70,000 km from the Moon. The DPC was an optional correction burn.
5. DPC to DRO Departure (DRD): The spacecraft coasts to the departure point of the DRO and performs the DRD burn.
6. DRD to Return Powered Flyby (RPF): The spacecraft coasts to the Moon and performs the RPF burn.
7. RPF to Entry Interface (EI): The spacecraft coasts to EI.

ASSUMPTIONS AND CONSTRAINTS

For off-nominal trajectories, the possible trajectories were constrained by the Orion spacecraft performance. Since Artemis I was a test flight, and there were many unknowns about the vehicle performance, the constraints were conservative.

Orion trajectory constraints[12,13] include:

- Eclipse durations less than 90 minutes to satisfy an Orion requirement.
- Arrival on the EI target line,[14] which resulted in a splashdown off the coast of San Diego.
- Downrange distance traveled by the spacecraft from EI to landing was between minimum and maximum bounds that varied depending on the location along the target line in order to prevent overheating.
- The spacecraft's perilune did not go below 100 km for thermal constraints.
- The spacecraft's velocity relative to the Earth at EI was at lunar-return levels.
- The time between burns was equal to at least 10 hours for thermal constraints.

TYPES OF OFF-NOMINAL TRAJECTORIES

In order to prepare for contingencies and allow the completion of high-priority objectives during each phase of the mission, off-nominal trajectories were designed for each phase of flight. The types of available off-nominal trajectories varied depending on the mission phase. For pre- or partial-TLI contingencies, alternate-mission trajectories were generated. Post-TLI contingencies could be TIG slips, delayed burns, or partial burns, in which the off-nominal trajectory would return to the nominal trajectory, or aborts, in which the trajectory would return Orion to Earth at a re-entry velocity sufficient to test the heat shield without prioritizing other objectives. In cases where Orion would become uncontrollable or have insufficient propellant to return, it would be disposed of.

Off-nominal trajectories were generated for multiple epochs within a launch window. Alternate missions, TIG slips, burn delays, and partial-burn cases were generated for each minute within the launch window. Abort cases were generated at 30-minute intervals through the launch window. Table 1 shows the approximate number of trajectories generated at one epoch for each type of off-nominal case.

Table 1: Approximate Number of Produced Off-Nominal Trajectories for One Launch Epoch

Off-Nominal Scenario	Aborts	TIG Slip	Burn Delay	Partial Burn	Alternate Mission	Disposal
# Trajectories	1500	30	50	200	100	10

Alternate Missions

Alternate missions allowed Artemis I to achieve some mission objectives in the event of a failure before the Orion-ICPS separation. Analysis for TLI failures was done with respect to burn-completion percentage, modeled as a function of burn time. These missions resulted in three types of trajectories; two Highly Elliptical Orbit (HEO) types and one lunar-flyby type. In the event of a single core-engine failure, the SLS would have placed Orion into a pre-targeted orbit. This failure scenario, Alternate MECO Target (AMT), fell into the ascent regime of flight and was not handled by the Orion mission-design team, so it will not be discussed in-depth in this paper. Table 2 shows the available alternate missions and their ranges of applicability.

Table 2: Alternate Mission Types

Alternate-Mission Type	Applicability Range	Description
AMT-Lo	Core Stage failure on ascent (<∼1 minute MET)	Low Earth orbit.
AMT-Hi Highly Elliptical Orbit	Core Stage failure on ascent (<∼3.5 minute MET)	Highly Elliptical Earth orbit.
AMT-Hi Lunar Flyby	Core Stage failure on ascent (<∼3.5 minute MET)	Lunar Flyby.
Low-Partial TLI	∼0-15% TLI completion	556-km circular Earth orbit.
Mid-Partial TLI	∼15-75% TLI completion	1806-km-perigee Earth orbit.
High-Partial TLI HEO	∼75-99% TLI completion	Highly elliptical Earth orbit.
High-Partial TLI Lunar Flyby	∼75-99% TLI completion	Lunar flyby.

- **AMT-Lo:** From launch until ∼00:01:04 Mission Elapsed Time (MET), a single core-stage-engine failure would have resulted in Orion being placed into a stable pre-targeted 311x356-km orbit, which would have allowed time to plan a contingency mission or deorbit. The core stage and ICPS would land in the Atlantic Ocean. After core separation, Orion would separate from the ICPS and would place itself into a 556-km circular orbit, where it would remain for as long as possible, given vehicle and orbit constraints, before deorbiting. Deorbit from Low Earth Orbit (LEO) would not achieve the heat-shield test.
- **AMT-Hi** From ∼00:01:04 to 00:03:25 MET, an engine failure would have resulted in the SLS inserting Orion into a 19×741-km orbit, after which the ICPS would raise the perigee to 187 km. ICPS would then perform as much of the TLI as possible, and Orion would either place itself into a Highly Elliptical Orbit or a lunar-flyby trajectory to achieve lunar-return velocities for the heat-shield test. If unable to achieve lunar-return velocities, Orion would maximize the EI velocity.
- **Low-Partial-TLI:** If the TLI burn were ∼0-15% complete, Orion would use two burns to insert itself into a 556-km circular orbit and use a third burn to deorbit. It would target an alternate target line near San Diego. This case achieved the time-in-space objective. Note that this case was not generated by the mission design team other than some proof-of-concept trajectories.
- **Mid-Partial-TLI:** If the TLI burn were between ∼15-75% complete, Orion would coast (shown in magenta in Figure 3a) and perform one burn near apogee to raise the perigee altitude to 1806 km. Orion would remain in the parking orbit (shown in blue in Figure 3a) between 7 to 30 days to allow nodal regression to align the orbit with the weather-alternate target region near San Diego and would then perform a deorbit burn (emphasized in Figure 3b by hiding the parking orbit) near apogee of the parking orbit. This mission achieved the time-in-space objective.
- **High-Partial-TLI, HEO:** If the TLI burn were between ∼75-99% complete, Orion could be placed into a HEO, similar to that for the AMT-Hi case. This case has two variations: a 'standard' variation for 75-96% TLI completion (Figure 3c), and a 'direct' variation for 97-99% TLI completion (Figure 3d). In the standard case, Orion would enter a coast orbit until at least 12 hours after TLI and perform a burn near perigee. For the direct case, the spacecraft would have enough energy such that it would be more efficient to perform the first burn right at 12 hours post-TLI along the outbound trajectory. In both cases, the second, much smaller, burn was performed near apogee and mainly served as a plane-change maneuver to target EI.

The EI MET for these missions was always near 8 days. Both variations achieved lunar-return velocities required for the heat-shield test.

- **High-Partial-TLI, Lunar Flyby:** If the TLI burn had been between ∼75-99% complete, Orion could have been placed on a lunar-flyby trajectory, constrained to pass within 70,000 km of the Moon. Similar to the highly-elliptical-orbit case, there were 'standard' (Figure 3e) and 'direct' variations (Figure 3f). This mission was a single-burn case, as a free-return lunar flyby was used to return the spacecraft to the nominal target line at an EI time between 9 and 15 days MET. This case satisfied the heat-shield and time-in-space objectives. Note that the post-TLI orbit was identical to the HEO case.

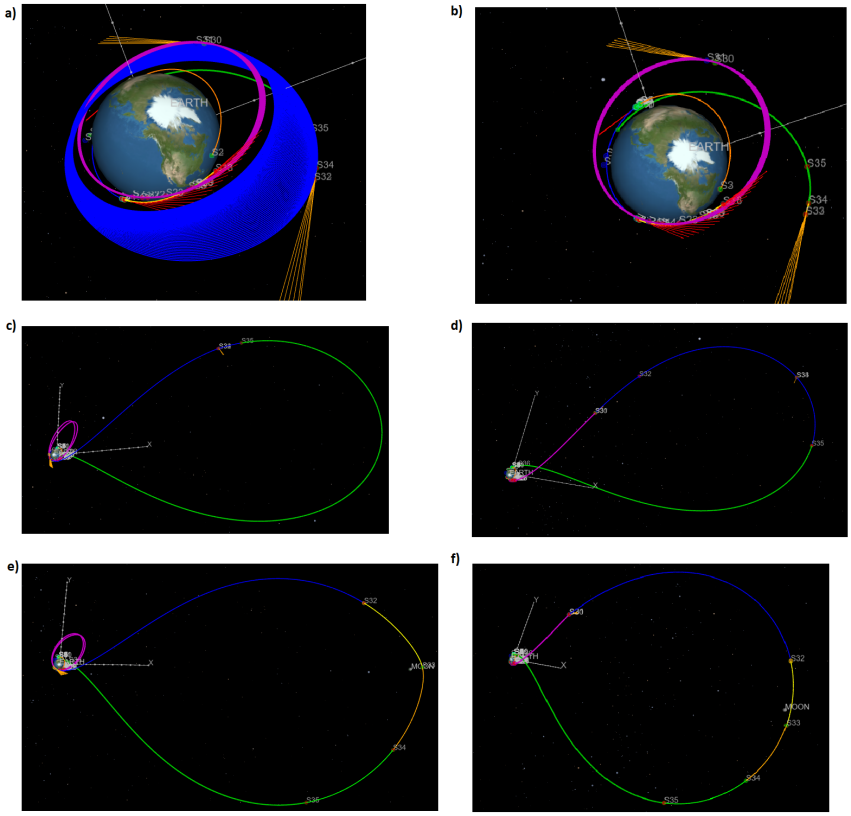

Figure 3: Alternate-mission trajectories. a) Mid-Partial-TLI orbit, parking orbit shown. b) Mid-Partial-TLI orbit, parking orbit hidden. c) Partial-TLI to HEO, standard. d) Partial-TLI to HEO, direct. e) Partial-TLI to Flyby, standard. f) Partial-TLI to Flyby, direct.

Missed-Burn Recoveries

Missed-burn recoveries are a sub-class of off-nominal scenarios where a major burn either does not execute at the planned TIG or does not complete as expected. Missed-burn recoveries plan a subsequent recovery burn to return Orion to the nominal trajectory and mission.

TIG-Slip Recoveries[15] were burns that did not occur at the planned TIG, but occurred while the spacecraft was still configured for a burn. The slips could have been caused by violations of burn-initiation constraints, such as the vehicle not being in the burn attitude. In the event of a TIG slip,

Orion would retain the original onboard targets. A subsequent correction burn could rectify any velocity discrepancy from the reference trajectory. For each major burn, TIG-slip recoveries were generated for slips of 5, 10, and 20 minutes.

Delayed-Burn Recoveries[15] were burns that were canceled and replanned for a later TIG. A burn could be delayed for several reasons, including operational and vehicle-constraint violations. As the nominal burn times were chosen to minimize propellant use, the delayed-burn recovery would increase in propellant usage with the length of the delay. A recovery burn could either target the next major burn and allow the major burn to re-optimize, or target the next minor burn and keep the next major burn fixed. Sufficient propellant was typically available to allow the burn to be delayed for hours or even a day, with the exception of powered lunar flybys. Delayed-burn recoveries were generated for each mission during the launch window for delays up to 36 hours. Burn-delay capability informed the impact of missing a major burn, which allowed the operations teams to configure burns to the correct redundancy.

Partial-Burn Recoveries[15] were recovery burns inserted after a burn was partially completed and were generated at each minute during the launch window for percentage-completion values from 0 to 95 and delays of 6, 12, 24 and 36 hours. The recovery burn could place Orion back onto the reference trajectory or re-optimize the subsequent mission.

Aborts

Aborts were performed when a problem jeopardized the vehicle's return. Since testing the spacecraft's heat shield was the highest mission priority, that objective was prioritized over completing other objectives. Abort trajectories were generated between TLI and RPF with combinations of input parameters (Table 3). The particular combination of input parameters determined the solution family for the abort trajectory.

Table 3: Abort Parameters

Parameter	**Options**
Abort Type	Direct, flyby, or missed-burn
Mission Phase	TLI to OPF, OPF to DRI, DRI to DPC, DPC to DRD, DRD to RPF
Engine	Orbital Maneuvering System Engine (OMSe) or 8 +X engines
Number of Burns	1 or 2
TIG for Abort Burn 1	12-hour increments between major burns
EI Day	Varies with case

Three types of abort trajectories were generated: direct, flyby, and missed-burn. A cutoff of 70,000 km from the Moon, the radius of the initial state of the Artemis I target DRO, was used to inform the division between direct and flyby aborts, though, in practice, the division was arbitrary. Aborts occurring after OPF were classified as flybys for simplicity.

Missed-burn aborts occurred after a major burn was not performed. Note that this case is different than the missed-burn recovery cases discussed in a previous section. In missed-burn recovery cases, the spacecraft returns to the nominal trajectory. In missed-burn-abort cases, the spacecraft returns to Earth without attempting to achieve mission objectives other than the heatshield test. Because a missed TLI would result in an alternate mission rather than an abort, all missed-burn aborts occurred from the time of OPF onward and were flyby aborts.

Figures 4 - 6 show the available solution families for each mission phase. For mission phases

with multiple solution families, the optimal solution family for a particular trajectory depended on the combination of input parameters mentioned earlier, as well as the launch epoch.

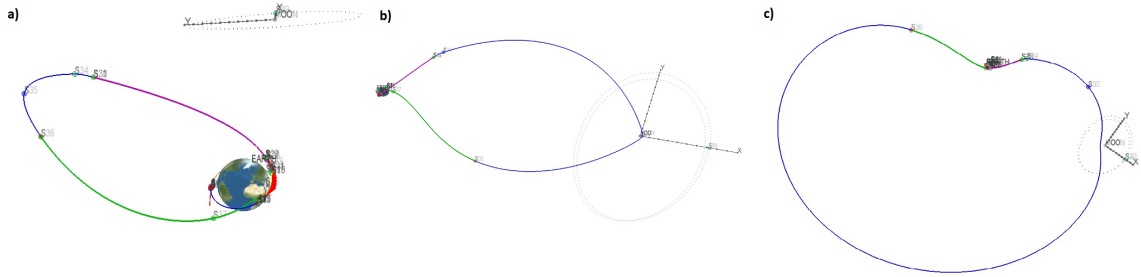

Figure 4: TLI-to-OPF abort families. a) Direct abort. b) Behind-the-Moon flyby abort. c) In-front-of-the-Moon flyby abort.

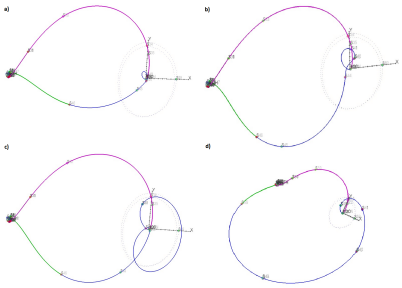

Figure 5: OPF-to-DPC abort families. a) Quick turnaround. b) Cut in front. c) Modified nominal. d) Far from Moon.

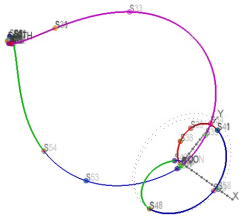

Figure 6: DRD-to-RPF abort family - modified nominal.

Abort trajectories minimized the total required delta-v of the abort burns subject to constraints for minimum perilune altitude, minimum final spacecraft mass, velocity at EI, and hitting the EI target line. Burn times, burn directions, coast times, and EI time and state were the control variables. In the event of an abort, the specific trajectory would have been selected based on criteria such as available fuel, available time, spacecraft-constraint violations, and recovery-ship availability.

Disposals

Permanent communications loss, imminent loss of attitude control, or insufficient fuel to return to Earth would have required Orion to be placed on a disposal trajectory. Table 4 gives the disposal options and their regions of applicability.

Table 4: Disposal Options

Disposal Option	Region of Applicability
DRO Disposal	Outbound Leg and in DRO
Earth-Atmosphere Burn-up	After RPF
Heliocentric Disposal	Between DRD and RPF
Lunar Impact	Between DRD and RPF

The stability of DROs meant Orion could remain in that orbit for decades without correction manuevers.[16] Therefore, for disposal situations between TLI and DRD, the chosen option was to either autonomously place Orion in the DRO or remain in the DRO. Since the actions in these situations would be to either perform the nominal OPF and/or DRI burns or to perform no further burns, no trajectories were generated specifically for this option.

After RPF, the only available disposal option was to place the spacecraft on a trajectory to burn up during reentry in Earth's atmosphere. Since this option would require an adjustment of the flight path angle after reaching EI, the flight controllers would have configured Orion for this condition, so trajectories were not generated specifically for this option.

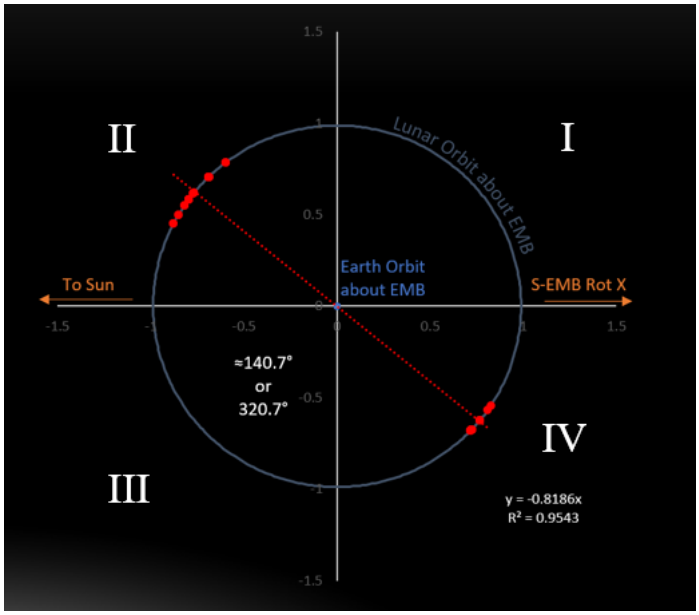

Figure 7: Lunar geometry at perilune of Monte Carlo disposal cases that fail to leave the Earth-Moon system or return to it in less than a decade with respect to the Sun-Earth/Moon-Barycenter(EMB) rotating frame centered on the EMB.

Between DRD and RPF, one available disposal option was using a one-burn trajectory to escape the Earth-Moon system and enter heliocentric space. The spacecraft's Jacobi constant for an Artemis I DRO in the Earth-Moon Circular Restricted Three-Body Problem was high enough to allow escape through either the L2 or L3 points, but the L2 point was targeted to reduce the risk of Earth impact and having to do the additional flyby of the Earth. Since the resulting orbit would have a tangent point to the Earth-Moon system, it would come into contact with that system in the future. In addition, the Sun/Earth/-Moon geometry of date, the Sun's gravity, and solar radiation pressure could also prevent escape or long-term evasion.[17]

A Monte Carlo analysis of attempted heliocentric disposals resulting in perilune passage was performed throughout a year and propagated for a century. It showed a clear trend of returns to the Earth-Moon system in less than a decade when the perilune flyby occurred with the Moon in Quadrant II or IV of an Earth-centered Sun-Earth rotating frame (Figure 7). Heliocentric disposal at that point in the mission also required a large delta-v for the large change in the line of apsides and the gravity-assist turn angle, so there were few occasions where this disposal could have been performed.

The other disposal option between DRD and RPF was a lunar impact. These options were inexpensive, since they were lowering the perilune altitude at RPF, until coming close to RPF. Therefore, lunar-impact burns would not be performed within six hours of RPF. Trajectories were not allowed to overfly or impact heritage sites, active sites, or sites of future landings (Figure 8). The disposal burn was targeted to have a lunar impact near the equator with selenocentric longitude east of 100°E and west of 120°W.

Due to insufficient time to develop the automation for generating these trajectories during pre-launch scans, lunar-impact and heliocentric disposal options were generated and analyzed after launch using templates created prior to flight. These templates were used to produce solutions with a disposal burn every 12 hours after DRD until RPF, including explicit options at the correction burns between DRD and RPF.

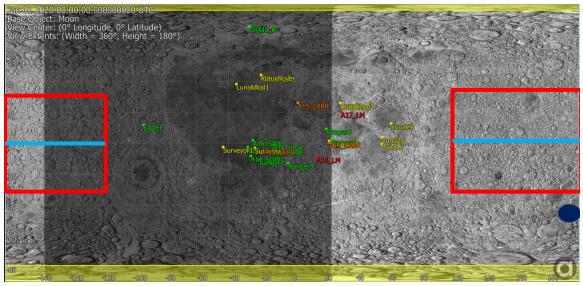

Figure 8: Lunar Keep-Out Zones for Disposal Planning. Red outlines: allowable impact region. Blue: Desired equatorial targets. Yellow: the regions of interest. Labeled points: the landing sites of previous missions. Blue oval: estimated range extent of Yutu-2.

[Credit: Charles Barrett and Randy Eckman, JSC]

RESULTS

Alternate Missions

Figure 9 shows the propellant usages across the different alternate missions for the launch epoch of 2022-11-16 0634 UTC, where the red boxes in the plots represent the point where missions exceed the allotted propellant. Notably, the spikes at 97% in Figures 9b and 9c represent the switch from the standard to direct variation of the respective missions. Spikes in Figure 9a are generally due to variations in the parking-orbit duration, resulting in varying deorbit-solution families. From a high level, achieving more of the TLI burn results in more energy in the trajectory and thus requires less delta-v to achieve the subsequent mission. This trend is seen across all plots, as an increase in this burn percentage results in a decrease to the total propellant usage.

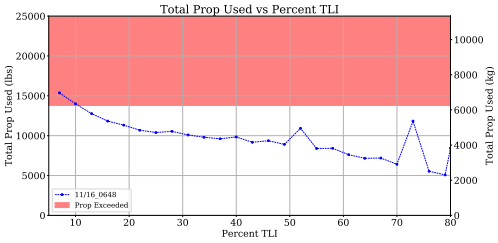

(a) Mid-partial TLI (Parking Orbit)

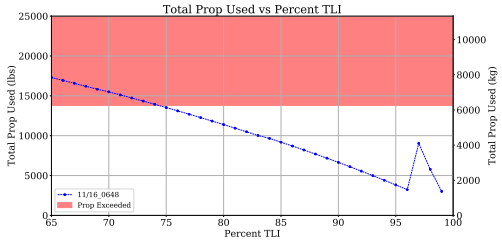

(b) High-partial TLI (HEO)

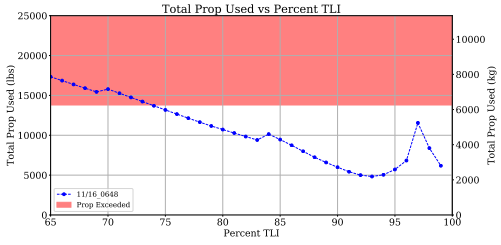

(c) High-partial TLI (Lunar-flyby)

Figure 9: Total propellant use for alternate missions across TLI percentage ranges (2022-11-16 0634 UTC)

The EI velocities are analyzed to verify the trajectories meet the heat-shield-test requirements. Examples of the inertial and relative velocities are shown for the high-partial TLI HEO cases in Figure 10.

Of most interest with alternate-mission analysis was to determine at what percentage of TLI completion a mission type became available (Figure 11). This knowledge allowed the Flight Operations team to define the alternate-mission space across a launch window. For each of these plots, a fixed propellant allocation was used to find the point at which the margin was greater than zero. Since these cases were run at integer-value percentages, the minimum percentages were calculated via interpolation. Since different numbers of revolutions were required for the mid-partial-TLI cases, the duration of the parking orbit varied frequently throughout the launch window and created greater variability in the minimum required percentage of TLI completion, observed in Figure 11a. The mid-partial-TLI cases all typically opened within the 12-18% range of TLI completion.

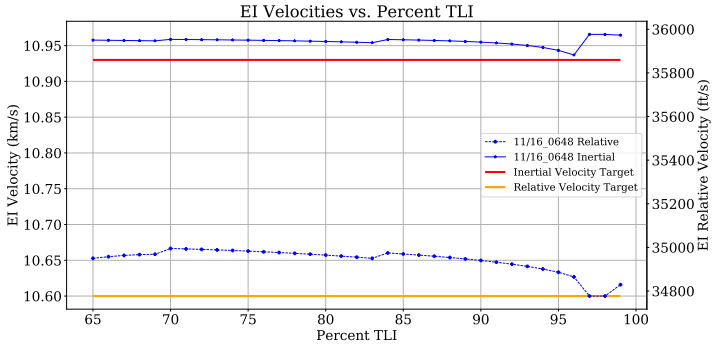

Figure 10: High-partial TLI (HEO) EI velocities across TLI percentage for the 2022-11-16 launch window.

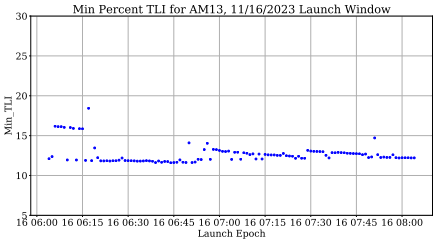

(a) Mid-partial TLI (Parking Orbit)

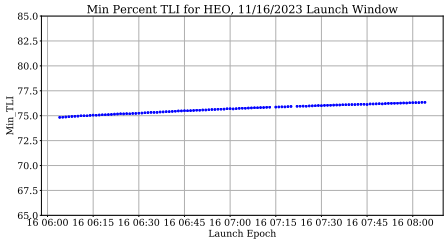

(b) High-partial TLI (HEO)

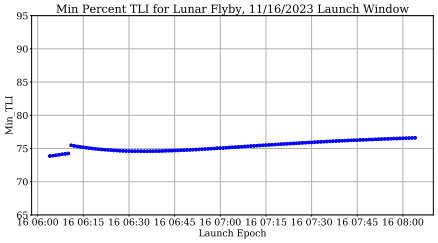

(c) High-partial TLI (Lunar-flyby)

Figure 11: Minimum TLI completion percentages across the 2022-11-16 launch window to achieve different alternate missions.

For the HEO missions (Figure 11b), a linear trend is seen with the percentage required to complete the mission, increasing about 2.5% through the window. This trend is typical for these cases due to

a minimal impact from Earth-Moon geometry.

The lunar-flyby mission space is shown in Figure 11c. The discontinuity about 10 minutes into the window is due to a jump to a different solution family, switching from about 10 days MET to 9 days MET. The trends in these cases typically have much more variation than the HEO mission due to the reliance upon the Moon. As seen for this launch window, the lunar-flyby case becomes available at a lower percentage of TLI completion, which can be counter-intuitive given the larger energy requirement to reach the Moon. Note, however, that this is a single-burn case, so a favorable flyby geometry can magnify the free-return effects and result in a lower delta-v cost.

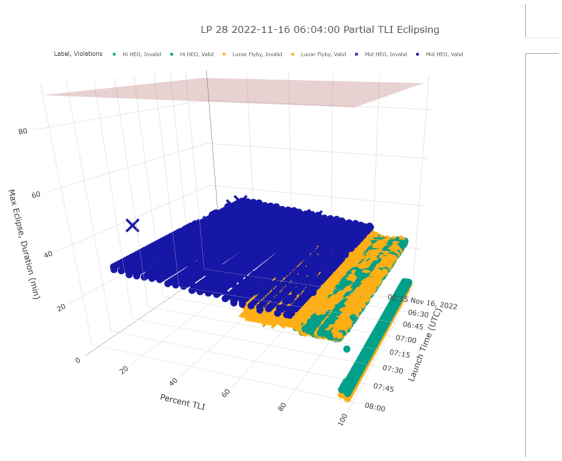

(a) Maximum eclipse durations for alternate missions.

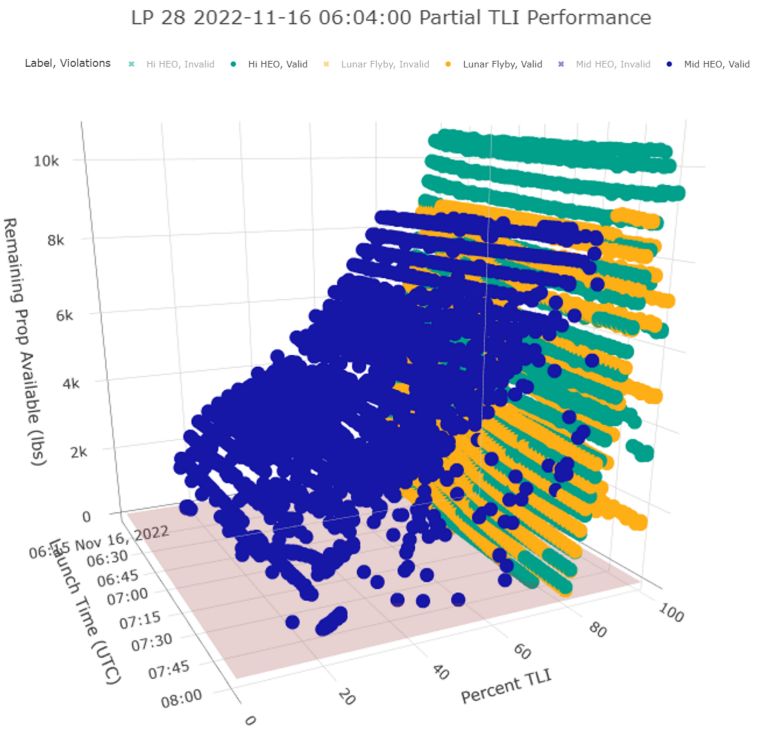

(b) All available alternate mission trajectories.

Figure 12: Alternate-Mission Results for the 2022-11-16 launch window.

These data are plotted together to show where mission capabilities exist (Figure 12b). These data demonstrate that if a TLI failure falls between 13-76%, there is mission coverage via the mid-partial-TLI, which is picked up around 76% by the two high-partial-TLI variations. For this particular window, a lunar flyby is more optimal and has a dense solution space, so this option would be chosen to cover the 76-99% range of failures. In other windows, this case didn't occur often, and a HEO would instead have been used for most, if not all, of this higher percentage range.

Finally, it is significant to analyze all solved alternate-mission trajectories for portions of the trajectory where Orion is continuously eclipsed for longer than 90 minutes. In some cases, a TLI failure may send Orion into a long eclipse, thus creating a loss-of-mission risk. Therefore, it is

necessary to find the longest eclipses for each alternate mission across a window. For 2022-11-16 (Figure 12a), none of the trajectories approach the 90-minute limit. For days when there are violations, they must either be mitigated or, in a worst-case scenario, would result in a launch-window cutout.

Missed-Burn Recoveries

As missed-burn-recovery cases continued the nominal mission, only a limited amount of propellant was available for the recovery burns. The maximum delay capability for the recovery burn for each case was determined based on the available extra propellant. All results presented are for pre-flight data for a launch epoch of 2022-11-16 0634 UTC. Note that, even though propellant capability might exist for longer delays, the maximum operational TIG slip was set as 20 minutes, and the maximum burn delay generated pre-flight was 36 hours. No results are presented for the DPC burn as DPC was not required for this trajectory.

TIG-Slip Results: All major burns have 20 minutes of TIG-slip capability for this launch epoch. This trend was found across all launch epochs, with the exception that OPF and RPF could have a limited TIG-slip capability for a propellant-stressing trajectory.

Burn-Delay Results: For this trajectory, all major burns that did not occur in a gravity well (Outbound Trajectory Correction (OTC)-1, DRI, DRD) could be delayed at least 36 hours. In order to delay 36 hours, re-optimized targets were necessary for the delayed burn. If returning to the nominal trajectory, DRI and DRD could only be delayed approximately 20 to 24 hours. This substantial delay capability makes these three burns non-critical, which means the burns can be delayed without impact to mission objectives and priorities. The major burns that occur near perilune (OPF and RPF) have no delay capability. These burns rely on the Oberth Effect, and any delay imposes a substantial performance cost. A missed OPF would have resulted in a missed-burn abort. A missed RPF would have resulted in potential loss of vehicle. The operational team used this information to apply a higher criticality to these burns and ensure redundancies were configured to maximize burn success. Figure 13 shows the extreme costs to an OPF or RPF delay, compared to lesser costs for the other major burns.

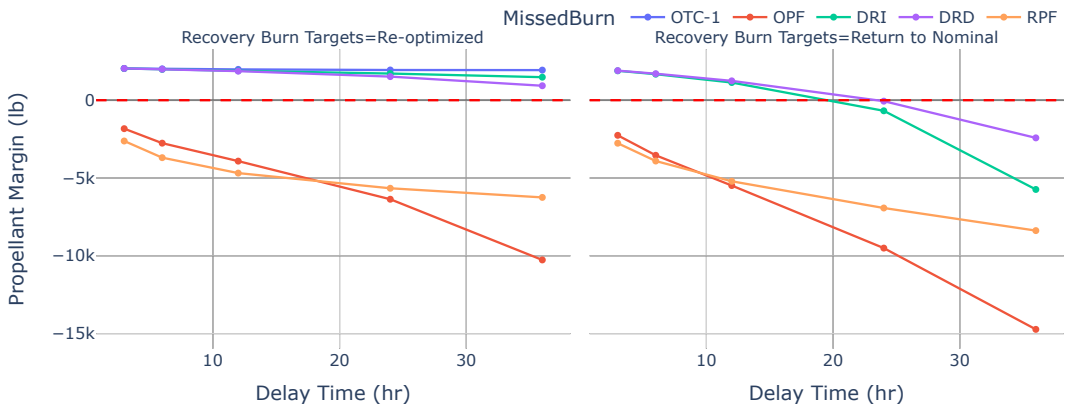

Figure 13: Remaining Orion Propellant Margin for Burn-Delay Scenarios

Partial-Burn-Recovery Results: Partial-burn-recovery performance was generally encompassed by burn-delay results (0% of burn completion) and the nominal burn (100% burn completion). Therefore, for the deep-space major burns that had a full 36 hours of delay capability, partial-burn analysis was unnecessary from a performance standpoint. It was still performed, however, to screen for other violations (e.g., eclipse). Figure 14 shows the remaining propellant margin after a partial-burn recovery. The powered flybys, which had no delay capability, do have partial-burn recovery capability. The recovery capability is dependent on the percentage of the original burn completed and the time between the partial burn and the recovery burn.

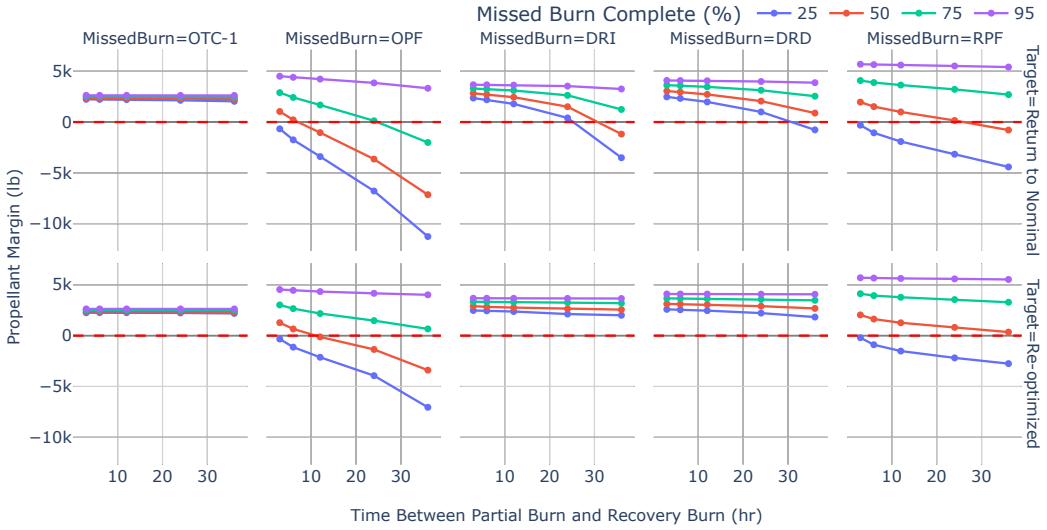

Figure 14: Partial Burn Recovery Cost for Various Burn Completion Percentages and Recovery Burn Targets

Aborts

Abort availability and delta-v were determined predominantly by the available combinations of TIG1 and the EI day, as seen in the following figures. Results are presented for the 2022-11-16 0634 UTC launch epoch, the closest epoch to the actual launch epoch for which pre-flight abort trajectories were generated. Only results for trajectories using the OMSe are presented. Results vary with launch epoch, sometimes significantly, but these results are sufficiently representative. Table 5 shows the delta-vs for the nominal mission for this launch epoch.

Table 5: Major Burns for the Nominal Mission for 2022-11-16 0634 UTC

Major Burn	Burn Delta-V (m/s)	Sum of Remaining Delta-Vs in Nominal Mission (m/s), Including Current Burn
OPF	178.681	727.411
DRI	110.490	548.730
DPC	0.000	438.240
DRD	145.136	438.240
RPF	293.104	293.104

Direct aborts provide the earliest return times (Figure 15a). Returning at four days MET is an option for early TIG1s, but not later times. In general, the ability to return on earlier EI days is lost for later TIG1s. The delta-v increases with lower EI day, particularly with combinations of earlier EI day and later TIG1.

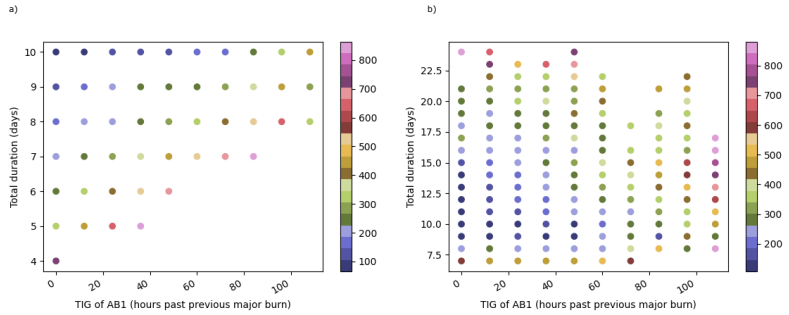

Figure 15: OTC1-to-OPF-abort delta-v for a launch of 2022-11-16 0634 UTC. a) Direct 2-burn aborts b) Flyby 2-burn aborts

Solution families in the following plots are given as a corresponding integer as defined in Table 6. Flyby aborts from OTC-1 to OPF (Figure 15b) are available for most combinations of TIG1 and EI. There is an area with lower delta-vs for the lower TIG1s and up to an EI day of 18.

For the OPF-to-DRI phase (Figure 16a), abort trajectories were not found for several TIG1 and EI combinations, either because the solution was not physically possible or because Copernicus was unable to find a trajectory with the given initial guess. It can be seen, by comparing Figures 16a and b, that the cheaper solutions are in the modified-nominal solution family, and the more expensive solutions are in the cut-in-front family.

Table 6: Abort Solution Families

Number	Solution Family
0	Direct
1	Post-OCO flyby behind the Moon
2	Post-OCO flyby in front of the Moon
3	Quick turnaround
4	Cut in front
5	Modified nominal
6	Far from Moon
7	Post-RPF EI adjustment

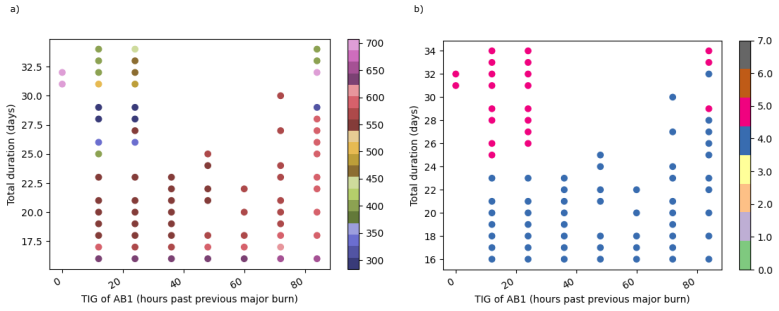

Figure 16: OPF-to-DRI aborts for a launch of 2022-11-16 0634 UTC. a) Delta-v b) Solution families

For flyby aborts between DRI and DPC (Figure 17a), DPC and DRD (Figure 17b), and DRD and RPF (Figure 17c), the delta-vs are within a narrow range regardless of the combination of TIG1 and EI. For this particular launch date, these trajectories are all in the modified-nominal family.

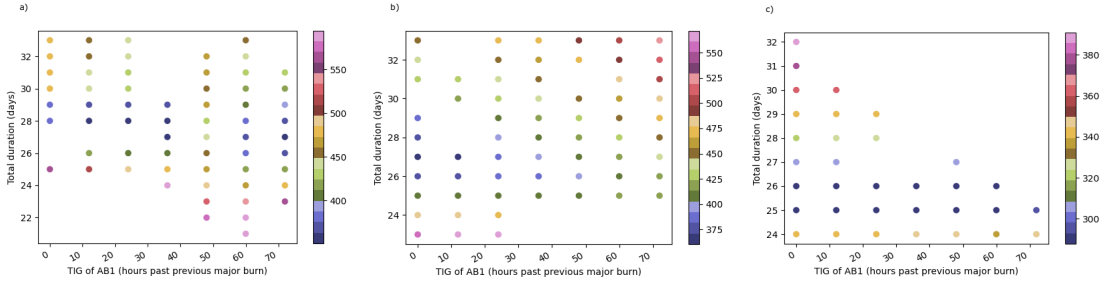

Figure 17: DRI-to-RPF flyby-abort delta-v for a launch of 2022-11-16 0634 UTC. a) DRI-DPC b) DPC-DRD c) DRD-RPF

Missed-burn-abort results are not shown, as the regular aborts are considered sufficiently representative for abort results. In general, missed-burn aborts have fewer available solutions in each mission phase.

Figure 18a shows the delta-v versus time between burns for aborts from OPF to RPF for flyby aborts. For most cases, the second abort burn has a higher delta-v than the first abort burn. Figure 18b shows the distance from the Moon's center for each burn. For most cases, with exceptions, the second abort burn is significantly closer to the Moon than the first burn. The implication is that the first burn is performed to set up an optimal location for the second abort burn, which is often near the Moon. The second burn, then, often takes the place of the nominal mission's return powered flyby.

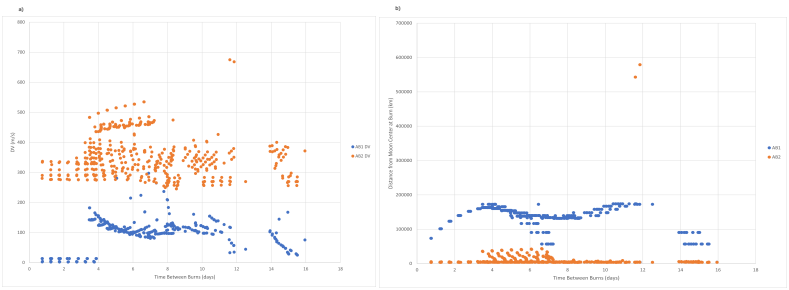

Figure 18: Delta-v and distance from the Moon vs. time between burns for flyby aborts for a launch epoch of 2022-11-16 0634 UTC. a) Delta-v b) Distance from the Moon at the time of the burn

Disposals

Specific trajectories were not generated for DRO-disposal or Earth-atmosphere-burnup options, but a limited number of lunar-impact and heliocentric-disposal trajectories were generated after

launch. The resulting plots of disposal-burn delta-v for the actual Artemis I launch epoch generated during the mission are shown in Figures 19 and 20.

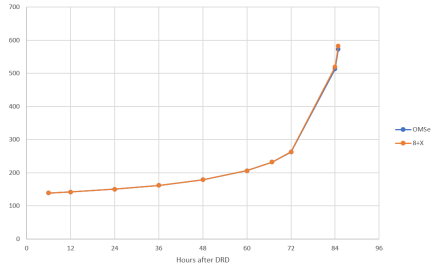

Figure 19: Lunar-impact delta-v in ft/s for the 2022-11-16 06:47:43.643 UTC launch.

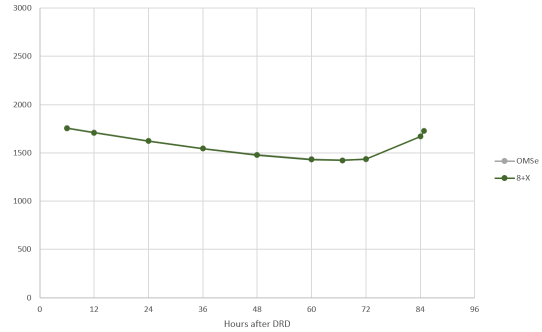

Figure 20: Heliocentric-disposal delta-v in ft/s for the 2022-11-16 06:47:43.643 UTC launch.

CONCLUSION

A variety of off-nominal trajectories were available for Artemis I, including returning to the nominal trajectory, alternate missions, and aborts. These off-nominal trajectories were subject to either a full or partial set of the constraints applied to the nominal mission and achieved some or all of the Artemis I mission objectives. As options were available throughout the flight, often with multiple options available during any given mission phase, the Orion spacecraft was capable of completing the highest-priority mission objectives in situations with a single fault. It was essential to achieve the highest-priority mission objectives on Artemis I in order to certify Orion as human-rated for Artemis II and beyond.

ACKNOWLEDGEMENTS

The authors wish to thank the many people who have contributed to the Artemis I mission design process, especially: Jeff Gutkowski, Amelia Batcha, Sarah Smallwood, Max Widner, Dave Lee, and Charlie Barrett. And thanks to Brian McCarthy for his independent technical review.

A portion of this work was funded by NASA JSC under contract NNJ13HA01C.

NOTATION

AMT	Alternate MECO Target
DAG	Directed Acyclic Graph
DPC	DRO Plane Change
DRD	DRO Departure
DRI	DRO Insertion
DRO	Distant Retrograde Orbit
EI	Entry Interface
EOP	Earth-Orientation Parameters
GRACE	Gravity Recovery And Climate Experiment
GRAIL	Gravity Recovery and Interior Laboratory
GUI	Graphical User Interface
HEO	Highly Elliptical Orbit
ICPS	Interim Cryogenic Propulsion Stage
IERS	International Earth Rotation Service
JPL	Jet Propulsion Laboratory
JSC	Johnson Space Center
LEO	Low Earth Orbit
MET	Mission Elapsed Time
NASA	National Aeronautics and Space Administration
OMSe	Orbital Maneuvering System Engine
OPF	Outbound Powered Flyby

OTC	Outbound Trajectory Correction	**SOFA**	Standards of Fundamental Astronomy
RPF	Return Powered Flyby	**TIG**	Time of Ignition
SLS	Space Launch System	**TLI**	Trans-Lunar Injection

REFERENCES

[1] F. D. O. Flight Operations Directorate, Trajectory Branch, "Artemis Flight Dynamics Officer Handbook CM-CH-10. Volume 1: All Mission Phases," Flight Dynamics Officer Handbook, NASA Johnson Space Center, Mar. 2021.

[2] J. Williams, "Copernicus Version 4.6 User Guide," User Guide, NASA Johnson Space Center, Apr. 2018.

[3] J. Williams, A. H. Kamath, R. A. Eckman, G. L. Condon, R. Mathur, and D. C. Davis, "Copernicus 5.0: Latest Advances in JSC's Spacecraft Trajectory Optimization and Design System," AAS/AIAA Astrodynamics Specialist Conference, Aug. 2019. AAS 19-719.

[4] P. E. Gill, W. Murray, and M. A. Saunders, "SNOPT: An SQP Algorithm For Large-Scale Constrained Optimization," *SIAM Journal on Optimization*, Vol. 12, 1997, pp. 979–1006.

[5] L. F. Shampine and H. A. Watts, "DEPAC – Design of a User Oriented Package of ODE Solvers," Tech. Rep. SAND-79-2374, Sandia National Labs, Sept. 1980.

[6] A. L. Batcha, J. Williams, T. F. Dawn, J. P. Gutkowski, M. V. Widner, S. L. Smallwood, B. J. Killeen, E. C. Williams, and R. E. Harpold, "Artemis I Trajectory Design and Optimization," 2020. AAS 20-649.

[7] W. M. Folkner, J. G. Williams, and D. H. Boggs, "The Planetary and Lunar Ephemeris: DE 421," Memorandum IOM 343R-08-003, Jet Propulsion Laboratory, California Institute of Technology, March 2008.

[8] B. Tapley, J. Ries, S. Bettadpur, D. Chambers, M. Cheng, F. Condi, B. Gunter, Z. Kang, P. Nagel, R. Pastor, T. Pekker, S. Poole, and F. Wang, "GGM02: An Improved Earth Gravity Field Model from GRACE," *Journal of Geodesy*, Vol. 79, 2005.

[9] IAU SOFA Board, "IAU SOFA Software Collection," http://www.iausofa.org.

[10] F. G. Lemoine, S. Goossens, T. J. Sabaka, J. B. Nicholas, E. Mazarico, D. D. Rowlands, B. D. Loomis, D. S. Chinn, D. S. Caprette, G. A. Neumann, D. E. Smith, and M. T. Zuber, "High-Degree Gravity Models from GRAIL Primary Mission Data," *Journal of Geophysical Research: Planets*, Vol. 118, No. 8, 2013, pp. 1676–1698.

[11] "A Standardized Lunar Coordinate System for the Lunar Reconnaissance Orbiter and Lunar Datasets, Version 5," tech. rep., NASA Goddard Space Flight Center, October 2008.

[12] NASA, "ESD 10042 - Cross Program End-to-End Performance Ground Rules and Assumptions for Artemis I, Revision E," Reference Document, NASA Johnson Space Center, Dec. 2021.

[13] F. O. Directorate, "Artemis Operational Flight Rules - Artemis I," Flight Rules, NASA Johnson Space Center, Oct. 2021.

[14] J. Rea, "Orion Exploration Mission Entry Interface Target Line," AIAA/AAS Space Flight Mechanics Meeting, Feb. 2016. AAS 16-485.

[15] B. Killeen, "EG-TARGO-19-06: Delivery of CFP-A FMA Missed DRD Burn (Return to Mission) Idecks," TARGO Memo, NASA Johnson Space Center, Oct. 2019. EG-TARGO-19-06.

[16] G. Turner, "Results of Long-Duration Simulation of Distant Retrograde Orbits," *Aerospace*, Vol. 3, No. 4, 2016, pp. 37–61.

[17] K. K. Boudad, D. C. Davis, and K. C. Howell, "Disposal Trajectories from Near Rectilinear Halo Orbits," AAS/AIAA Astrodynamics Specialists Conference, Aug. 2018. AAS 18-289.